Published in final edited form as:
Childs Nerv Syst. 2012 September ; 28(9): 1483–1493. doi:10.1007/s00381-012-1778-9.

Phenotype profile of a genetic mouse model for Muenke syndrome

Hyun-Duck Nah,
Plastic and Reconstructive Surgery, University of Pennsylvania Perelman School of Medicine, Philadelphia, PA 19104, USA

Plastic and Reconstructive Surgery, The Children's Hospital of Philadelphia, 1116G/ARC, 3615 Civic Center Blvd, Philadelphia, PA 19104, USA

Eiki Koyama,
Orthopaedic Surgery, The Children's Hospital of Philadelphia, University of Pennsylvania Perelman School of Medicine, Philadelphia, PA 19104, USA

Nneamaka B. Agochukwu,
Medical Genetics Branch, National Human Genome Research Institute, National Institutes of Health, Bethesda, MD, USA

Clinical Research Training Program, National Institutes of Health, Bethesda, MD, USA

Scott P. Bartlett, and
Plastic and Reconstructive Surgery, University of Pennsylvania Perelman School of Medicine, Philadelphia, PA 19104, USA

Maximilian Muenke
Medical Genetics Branch, National Human Genome Research Institute, National Institutes of Health, Bethesda, MD, USA

Hyun-Duck Nah: nah@email.chop.edu

Abstract

Purpose—The Muenke syndrome mutation (*FGFR3*^{P250R}), which was discovered 15 years ago, represents the single most common craniosynostosis mutation. Muenke syndrome is characterized by coronal suture synostosis, mid-face hypoplasia, subtle limb anomalies, and hearing loss. However, the spectrum of clinical presentation continues to expand. To better understand the pathophysiology of the Muenke syndrome, we present collective findings from several recent studies that have characterized a genetically equivalent mouse model for Muenke syndrome (*FgfR3*^{P244R}) and compare them with human phenotypes.

Conclusions—*FgfR3*^{P244R} mutant mice show premature fusion of facial sutures, premaxillary and/or zygomatic sutures, but rarely the coronal suture. The mice also lack the typical limb phenotype. On the other hand, the mutant mice display maxillary retrusion in association with a shortening of the anterior cranial base and a premature closure of intersphenoidal and spheno-

Correspondence to: Hyun-Duck Nah, nah@email.chop.edu.

occipital synchondroses, resembling human midface hypoplasia. In addition, sensorineural hearing loss is detected in all *FgfR3*^{P244R} mutant mice as in the majority of Muenke syndrome patients. It is caused by a defect in the mechanism of cell fate determination in the organ of Corti. The mice also express phenotypes that have not been previously described in humans, such as reduced cortical bone thickness, hypoplastic trabecular bone, and defective temporomandibular joint structure. Therefore, the *FgfR3*^{P244R} mouse provides an excellent opportunity to study disease mechanisms of some classical phenotypes of Muenke syndrome and to test novel therapeutic strategies. The mouse model can also be further explored to discover previously unreported yet potentially significant phenotypes of Muenke syndrome.

Keywords

Muenke syndrome; Genetic mouse model; FGFR3

Introduction

Muenke syndrome is an autosomal dominant disorder with prevalence of one in 30,000 births [5]. It is characterized by uni- or bilateral coronal suture synostosis (bilateral more often than unilateral), dysmorphic craniofacial features, macrocephaly without craniosynostosis, sensorineural hearing loss, intellectual disability, developmental delay, brachydactyly, coned epiphyses and carpal and tarsal bone fusions [13, 16, 17, 36] (Fig. 1). The craniofacial features include facial asymmetry, hypertelorism, downslanting palpebral fissures, ptosis of the eyelids, temporal bossing, dental malocclusion, a highly arched palate and midfacial hypoplasia [1, 13, 16, 17, 36] (Fig. 1). However, clinical diagnosis of Muenke syndrome can be challenging due to incomplete penetrance and variable expressivity of the phenotype. Considerable phenotypic variability occurs even within the same family [10, 14]. Some individuals with Muenke syndrome may have no signs of Muenke syndrome on physical or radiographic examination. The Muenke syndrome phenotype overlaps with other craniosynostosis syndromes, such as Saethre-Chotzen, Pfeiffer, and Crouzon syndrome. Diagnosis of Muenke syndrome is established by genetic testing for the presence of the defining Pro250Arg/P250R (c.749C > G) mutation in the *Fibroblast Growth Factor 3* (*FGFR3*) gene [4, 36]. This particular mutation accounts for about 8 % of all patients with craniosynostosis and 25–30 % of patients with craniosynostosis and a genetic cause; thus, this mutation in *FGFR3* represents the single most common craniosynostosis mutation [32, 33, 52]. To study the pathophysiology of Muenke syndrome, Twigg et al. [50] have generated the genetic mice harboring the gene mutation responsible for the Muenke syndrome (*FgfR3*^{P244R}). The P244R substitution in mouse FgfR3 is equivalent to the P250R substitution in human FGFR3. So far, the genetic mouse model has been characterized in four studies for skeletal and craniofacial phenotypes and hearing loss [25, 27, 50, 54]. In this report, we will first briefly introduce the structure and function of FGFR3. We will then review and discuss the findings from the genetic mouse model and compare them with human phenotypes.

Fibroblast growth factor receptor 3 (FGFR3): functions and mutations

FGFR3 is a member of the highly conserved FGFR family, which belongs to a superfamily of tyrosine kinase transmembrane receptors. FGFRs are encoded by four genes, *FGFR1–4*. FGFRs are high affinity receptors of a large family of fibroblast growth factors. FGFRs share a common structure that consists of an extracellular ligand-binding domain containing three immunoglobulin-like loops (IgI–III), a transmembrane domain and a split intracellular tyrosine kinase domain (Fig. 2a). FGFRs are produced in alternatively spliced forms, which display tissue-type and ligand-binding specificity [41]. Exons 8 and 9, which encode the second half of the IgIII domain of FGFR1–3, are alternatively spliced in a tissue-specific manner, generating the epithelial tissue-specific IIIb form and the mesenchymal tissue-specific IIIc form (Fig. 2b) [6]. In skeletal tissues, FGFR1 and 2 IIIc forms are expressed in bone tissue, whereas FGFR3 IIIc is expressed highly in cartilage and at low levels in the cranial suture mesenchyme [12, 41, 44]. In the auditory system, FGFR3 IIIc is expressed in cochlea [42]. Upon binding to FGF ligands, FGFRs form dimers, which in turn induce auto/trans-phosphorylation of the intracellular tyrosine kinase domains of one receptor molecule by the other. The phosphorylated FGFRs then activate a complex array of biochemical and molecular signaling pathways to transduce auto-/paracrine FGF signals in target cells.

FGFR3 is highly expressed in the proliferating zone of the epiphyseal growth plate [9, 12], which is the primary growth center that drives longitudinal growth of the long bone by endochondral ossification. Loss of FGFR3 activity was found to associate with increased rates of chondrocyte proliferation and lengthened chondrocyte columns in the *FgfR3* null mouse epiphyseal growth plate. Conversely, knock-in mice harboring ligand-independent constitutively activating *FgfR3* mutations showed decreased chondrocyte proliferation and differentiation associated with a profound affect on long bone growth [12, 29, 38, 39]. Consistent with the findings from animal studies, the mutations leading to ligand-independent phosphorylation and activation of the FGFR3 are causally linked to deficient long bone growth in the most common form of dwarfism, achondroplasia (G380R), and hypochondroplasia (N540K), and also a severe lethal form of skeletal dysplasia, thanatophoric dysplasia (R248C, S249C, G370C, S371C, Y373C, L650E) in humans [2, 3, 35, 46]. Constitutively active FGFR3 inhibits chondrocyte proliferation by dysregulation of the Indian hedgehog (IHH)-parathyroid hormone related peptide (PTHrP) feedback signal [7] and STAT signaling pathways [23]. Sustained activation of the MAPK pathway, which is expected from the constitutively active mutant FGFR3, has also been shown to inhibit chondrocyte differentiation and arrest endochondral bone growth [37, 55]. Constitutively active FGFR3-mediated signaling pathways, therefore, inhibit chondrocyte proliferation and differentiation and induce apoptosis (Fig. 2c).

Muenke syndrome is unique among skeletal dysplasias caused by FGFR3 dysfunction in that long bone growth appears to be largely unaffected. Rather, its primary effect is abnormal suture formation and defective limb morphogenesis [17, 24, 43, 47]. The clinical distinction between Muenke and other FGFR3-related syndromes may be explained by the unique molecular behavior of the FGFR3 protein harboring the defining Muenke syndrome mutation. A study using surface plasmon resonance and X-ray crystallography showed that the P250R mutation significantly enhanced FGFR3IIIc's affinity for un-natural ligands,

including FGF2 and FGF9, as well as one of its cognate ligands, FGF1 [20]. The calvarial suture phenotype in Muenke syndrome is shared with Apert and Pfeiffer syndromes, which are caused by the P253R mutation of FGFR2 (in 33 % of cases of Apert syndrome) and the P250R mutation of FGFR1 (in type I Pfeiffer syndrome), respectively. The Pro to Arg substitutions also endow FGFR2IIIc and FGFR1IIIc with the ability to bind FGF9 with high affinity [20, 51]. Given that FGF9 is highly expressed in the cranial suture and increased FGF9 signaling causes craniosynostosis in mutant mice (Eks) [18] and humans [53], aberrant FGFR signaling and subsequent hyperactive FGF9 signaling in the cranial suture may be the common molecular etiology that underlies these three craniosynostosis syndromes (Muenke, Apert, and Pfeiffer syndromes).

Craniofacial phenotype of the *FGFR3^{P244R}* mouse

Craniofacial sutures: synostosis

Craniosynostosis is present in 86 % of patients with Muenke syndrome. Of these patients, 55 % have bilateral coronal synostosis and 26 % have unilateral coronal synostosis. About 4 % of cases involve additional cranial sutures. The penetrance is 88 % for females and 76 % for males, with females two times more likely than males to have a severe phenotype: for example, females are more likely than males to have bilateral coronal synostosis vs. unilateral coronal synostosis. In females, the prevalence of bilateral coronal synostosis is more than two times the prevalence of unilateral coronal synostosis [13, 19, 24]. The presence of the FGFR3 P250R mutation is the single most predictable factor for increased risk of repeated transcranial surgery for raised intracranial pressure in patients with isolated coronal synostosis [49]. In addition, following the initial cranial remodeling surgery in infancy, Muenke syndrome patients invariably require secondary and tertiary surgical procedures for improved aesthetics [19]. Therefore, molecular confirmation of the defining mutation in *FGFR3* is essential for the planning and management of patients with Muenke syndrome.

Similar to humans, the *FgfR3^{P244R}* mouse model of Muenke syndrome showed incomplete penetrance of the phenotype. However, the gender bias was reversed in the mouse model. Male mice presented markedly abnormal skull shape in 100 % of homozygotes and about 25 % of heterozygotes, while female mice showed the phenotype in about 33 % of homozygotes and no phenotype in heterozygotes [50]. *FgfR3^{P244R}* mice with abnormally shaped heads showed characteristic loss of interdigitation and/or fusion of the premaxillary sutures and class III malocclusion of the incisors as early as postnatal week 1 [25, 50]. A dome-shaped and short skull with snout deviation, resembling asymmetric plagiocephaly, became pronounced in mutant mice at week 3 or later in the direction of the fused premaxillary suture (Fig. 3d). In mice with bilaterally fused premaxillary sutures, snouts were either shortened without deviation or deviated in the direction of the more severely disrupted premaxillary suture (Fig. 3d, f). In all of these cases, the premaxilla was visibly hypoplastic (Fig. 3e). Twigg et al. [50] reported that the zygomatico-maxillary suture was also fused in the majority of mutant mice that exhibited the skull phenotype [50]. Mutant mice presented with a broadened cranial base and an increased distance between orbits, resembling hypertelorism in human patients. While the *FgfR3^{P244R}* mouse model displays

many characteristic features of Muenke syndrome, coronal synostosis was rarely observed. The incidence was reported only in a few heterozygous mutant mice bred into a specific background (C57BL/6)[50]. Further studies are needed to clarify why the coronal suture is drastically less susceptible to the Muenke syndrome mutation than other sutures in mice.

Cranial base: premature closure of synchondroses

Mild to moderate midface hypoplasia with a depressed nasal bridge, a phenotype typically associated with deficient growth of the anterior cranial base, has also been reported in 50–70 % of patients with Muenke syndrome [13, 17, 45]. Comparison of the craniofacial phenotype between patients with Muenke syndrome and patients without Muenke syndrome with unilateral coronal synostosis showed that the severity of the craniofacial asymmetry was significantly greater in the patients with Muenke syndrome than those without Muenke syndrome, and was especially prominent in the anterior part of the skull and facial skeleton [22]. This suggests that the Muenke mutation might have a direct effect on cranial base growth.

The cranial base is composed of the frontal, ethmoid, sphenoid, and basioccipital bones along with otic vesicles, the petrous part of the temporal bone between the sphenoid and basioccipital bones (Fig. 4g), and develops largely by endochondral ossification. In embryos, the cranial base initially appears as a sheet of condensed mesenchyme, from which numerous cartilages arise. These cartilages grow and coalesce to form a confluent cartilagenous cranial base. Subsequently, endochondral ossification starts at discrete foci to form bones. The residual cartilage interposed between two bony elements, the synchondrosis, serves as the major growth site for the longitudinal growth of the cranial base. It has a unique bidirectional structure where two opposing growth plate cartilages share a zone of resting chondrocytes. There are many synchondroses located in the cranial base, and the age at which they close varies widely. The intersphenoidal (ISS) and spheno-occipital synchondroses (SOS) are the primary postnatal growth centers for the cranial base. The ISS closes between 2 and 3 years of age and the SOS closes much later, between 14 and 18 years of age [26, 40]. Closure of the SOS marks the end of significant cranial base growth and midface development.

Using the knock-in mouse model for Muenke syndrome (*FgfR3*^{P244R}), we have studied the cranial base phenotype of Muenke syndrome in detail [25]. Morphometric analyses revealed the mutant gene exerts a dose-dependent effect on the shortening of the basicranial length from postnatal week 3 onwards. Measurements for individual basicranial bones revealed significantly shortened presphenoid and basisphenoid bones in mutant mice. The length of the basioccipital bone was not affected by the mutation. Interestingly, a study using cell lineage-specific genetic markers showed that ethmoid and sphenoid bones are neural crest derived, while the basioccipital bone originates from the mesoderm [30]. Whether the cells of the neural crest origin are more susceptible to the Muenke syndrome mutation needs to be verified. μCT of basicranial synchondroses showed bony bridge formation in *FgfR3*^{P244R} mutants as early as postnatal week 3, but never in wild type juvenile mice (Fig. 4a–c). Bridge formation in *FgfR3*^{P244R} mutants was more prominent in the ISS than the SOS (Fig. 4). Homozygous (90 %) and heterozygous (40 %) mutants had formed bone across the ISS

by week 3, whereas only 30 % of homozygous and no heterozygous mice had bridging across the SOS at this time point (Fig. 4b, c). By week 5, 100 % of homozygous and 50 % of heterozygous mutant mice had ossification across the ISS, while 60 % of homozygous and 15 % of heterozygous mutant mice had bony bridging across the SOS (Fig. 4e, f). In contrast, ISS and SOS remained patent through week 5 in all wild type controls (Fig. 4d). Both synchondroses fully close after week 8, irrespective of genotype. These data indicate that longitudinal growth of the basicranium is ceasing or has ceased for most homozygous mutant mice by postnatal week 5, which is much earlier than unaffected wild-type mice.

The *FgfR3*^{P244R} mutation disrupts and shortens the growth plate in both ISS and SOS by disruption of the Indian hedgehog (IHH)-PTHrP feedback loop that maintains the population of proliferating chondrocytes [25]. Thus, in mutant synchondroses, the proliferating chondrocyte population is significantly reduced (Fig. 5a). In addition, resting chondrocytes in mutant synchondroses prematurely form the secondary ossification center populated with *CTGF* expressing prehypertrophic chondrocytes (Fig. 5a). The mutation also accelerates perichondreal ossification, resulting in bony bridge formation across the synchondrosis (Fig. 5b). It is quite possible that FGFR3-mediated signaling directly stimulates osteogenic differentiation of progenitor cells in the perichondreal region. This notion is supported by earlier studies showing FGF/FGFR induction of BMP/TGFβ gene expression in osteogenic cells [15], and essential roles of BMP/TGFβ signaling in osteoblast differentiation in the perichondrium [28, 31]. Activation of Erk-1/2, a downstream mediator of FGF/FGFR3 signaling, has also been shown to stimulate osteoblast differentiation and ossification of the perichondrium [29].

Cephalometric analyses of patients with Muenke syndrome show significant anterior cranial base shortening, averaging 8.4 mm in length [45]. As in the mouse model, premature fusion of basicranial synchondroses likely contributes to the anterior cranial base deficiency in patients. However, due to deficient human CT data, this is difficult to verify. Interestingly, although midface hypoplasia is reported in a majority of Muenke syndrome patients, less than 25%of the patients require midface advancement surgeries [8, 19]. This may be explained by the fact that Muenke syndrome patients are heterozygotes. In the mouse model, the phenotype was clearly dependent on the dose of the mutant gene. Also, mild midface hypoplasia can be dentally compensated, not requiring surgical correction. Another explanation is retardation of mandibular antero-posterior growth that essentially camouflages a mild midface hypoplasia. In fact, cephalometric measurements showed that Muenke patients had shorter mandibular body length than normal individuals by an average of 12.9 mm [45]. In conclusion, the Muenke syndrome mutation negatively affects cranial base growth as a result of growth plate dysfunction and accelerated perichondrial ossification in the basicranial synchondrosis.

Temporomandibular joint: defective development and arthritic changes

The temporomandibular joint forms between the mandibular condyle and the glenoid fossa of the temporal bone, which are intercalated by a fibrocartilaginous disc. In mammals, the mandibular condyle is a major site of growth. The condyle develops as secondary cartilage within the periosteal tissue of the developing mandible. As the cartilage grows, cells

organize themselves to form a growth plate-like structure. In *FgfR3*^{P244R} mice, the condylar head was underdeveloped, which was characterized by a significant shortening of its anterior half (Fig. 6a, b) [54]. The missing region normally contains rapidly dividing progenitor cells. Postnatal development of the temporomandibular joint is also disturbed in mutant mice. In 3-week-old mutants, condylar cartilage showed drastically reduced *Ihh* expression, which was accompanied by decreased chondrocyte proliferation and differentiation and defective formation of the primary bone spongiosa and trabecular bone (Fig. 6c–f) [54]. These changes are similar to those observed in mutant mouse basicranial synchondroses. Defective development of the mandibular condyle may explain deficient mandibular growth in Muenke syndrome patients. In addition to developmental defects, the condylar cartilage showed arthritic changes, including fissure formation and adhesion of the disc to the condylar surface and/or glenoid fossa (Fig. 6g, h) [54].

Generalized skeletal dysplasia

The characteristic limb phenotypes of Muenke syndrome, such as brachydactyly, coned epiphyses, and carpal/tarsal bone fusions, are missing in *FgfR3*^{P244R} mice, while the trunk skeleton appears normal. Even in mutant mice with abnormally shaped skulls, long bone growth is largely unaffected and the epiphyseal growth plate appears histologically normal [50]. However, micro CT analyses of the femora revealed that there was a 40 % reduction in cortical bone thickness and a 34 % reduction in bone mineral density in mutant mice compared to wild-type controls [50]. Skull bone thickness was also significantly reduced in mutant mice [50]. In the cranial base, although perichondrial ossification was accelerated across the synchondrosis, primary spongiosa, and trabecular bone formation was visibly defective in mutant mice older than 3 weeks of age [25] (Fig. 5). Therefore, the Muenke syndrome mutation resulted in generalized skeletal dysplasia in mice, affecting both cortical and trabecular bone formation. Considering that FGFR3 is expressed in preosteogenic mesenchymal stem cells, deficient bone formation in mutant mice is not surprising. So far, skeletal dysplasia has not been documented in patients with Muenke syndrome. If this phenotype is present in patients, it would likely be mild at young ages and become more pronounced with aging.

Sensorineural hearing loss

A review of all Muenke syndrome cases reported in the literature before 2007 found that the overall prevalence of associated hearing loss was about 40 % [13]. More recent studies however, find a much higher incidence of hearing loss, ranging from 62 % to 95 % [11, 13, 27]. Hearing loss in patients with Muenke syndrome is typically mild to moderate and predominantly characterized by sensorineural hearing loss at low frequencies [11, 13, 27]. The prevalence of hearing loss is also high in other craniosynostosis syndromes. A recent survey of young patients (aged between 4 and 18) with syndromic craniosynostosis (patients surveyed were patients with Apert, Crouzon, and Saethre-Chotzen syndrome) who had undergone audiometric assessment showed that mild to moderate hearing loss was found in 44 % of patients with Apert syndrome, 29 % of patients with Crouzon syndrome, and 28 % of patients with Saethre-Chotzen syndrome [11]. The etiology of hearing loss in these craniosynostosis syndromes was found to be largely conductive in origin due to inner ear

structural anomalies [11, 56]. Thus, the pathological mechanism underlying the hearing impairment of Muenke syndrome is distinctly different from that of other craniosynostosis syndromes.

Mansour et al. [27] have characterized the *FgfR3*^{P244R} mice and have shown that these mice have a sensorineuronal hearing loss that is most profound at low frequencies with high frequency sparing, a pattern similar to that observed in patients with Muenke syndrome. Hearing loss in the mouse model was dominant and fully penetrant and more severe than in humans. Although sensorineuronal hearing loss may be due to anomalies of the vestibulocochlear nerve, which innervates the cochlea and central auditory processing centers in brain, it is most commonly associated with dysfunction of the organ of Corti, the highly specialized sensory epithelium of the cochlea in the inner ear. In both humans and mice, the organ of Corti is composed of precisely organized rows of sensory hair cells and several types of support cells along the basilar membrane. Three outer rows of sensory hair cells are separated from a single inner row by two rows of pillar cells. The outer hair cells are supported by Deiter's and Hensen's cells, while inner hair cells are supported by phalangeal cells. A unique feature of the mammalian cochlea is the presence of the tunnel of Corti, a triangular fluid-filled extracellular space lined with pillar cells in the intervening region between the inner hair cell row and the first outer hair cell row. The intricate cellular architecture of the organ of Corti is essential for normal mechanosensory transduction in cochlea initiated by sound pressure.

FGFR3-mediated signaling has been shown to be necessary for the development of pillar cells. Within cochlea, the IIIc isoform of FGFR3 is expressed in progenitors that eventually differentiated into pillar cells, outer hair cells, Deiter's cells and Hensen's cells [21, 34, 42]. As the progenitors differentiate, FGFR3 expression becomes restricted to future pillar cells and is downregulated in the other cell types, suggesting a role for FGF signaling in cell fate determination [34]. FGF8, which is expressed in inner hair cells, is the principal ligand for FGFR3 during the induction of pillar cells [21]. Various genetic manipulations that change FGFR3 expression level or activation have shown to affect the number and differentiation of pillar cells. A targeted disruption of the *FgfR3* gene caused failed development of pillar cells and the tunnel of Corti [9]. In contrast, targeted deletion of *Spry2*, a negative modulator of FGFR3 signaling in differentiating pillar cells, caused their excess differentiation and converted Deiter's cell to a pillar cell fate with the ectopic formation of an extra tunnel of Corti [48]. Both *FgfR3* and *Spry2* null mice are deaf [9, 48].

Mansour et al. [27] found that *FgfR3*^{P244R} mice share a similar phenotype with *Spry2* null mice, which is characterized by excess pillar cell development at the expense of Deiter's cell development. Alterations in cell fate were observed along the entire length of the cochlear duct, with the most extreme abnormalities occurring in the apical (low-frequency) end. They also noted excess outer hair cell development in the apical region. These cellular changes are consistent with low-frequency sensorineural hearing loss. Thus, the *FgfR3*^{P244R} mutant mouse is an excellent model for studying hearing loss in Muenke syndrome. Mansour et al. [27] made an attempt to rescue this phenotype in *FgfR3*^{P244R} mutants by removal of a single copy of either *Fgf8* or *Fgf9* or both; however, this did not rescue hearing loss. It is possible that activation of mutant FGFR3 requires extremely low levels of ligand, or alternatively,

there may be ligands with redundant function available to pillar cells. Future studies may aim to inhibit mutant FGFR3 signaling by targeting downstream signaling intermediates or regulators.

Summary

Initial characterization of the *FgfR3*^{P244R} knock-in mouse model for the Muenke syndrome (*FgfR3*^{P244R}) has revealed that they present with premature fusion of a facial suture (premaxillary and/or zygomatic sutures instead of coronal suture), shortening of the cranial base/midface hypoplasia, and sensorineural hearing loss, mimicking the human phenotype of Muenke syndrome. This mouse model provides significant insight into the pathophysiological mechanism of hearing loss in patients with Muenke syndrome. Interestingly, phenotypes that have not been previously described in humans, such as reduced cortical bone thickness of long bones, hypoplastic cranial base trabecular bone, and progressive destruction of the temporomandibular joint structure, were found in the mouse model of Muenke syndrome. Given that new clinical findings are still being added to the description of Muenke syndrome, due to its fairly recent discovery, it is quite possible that the newly discovered phenotype may be present in human patients. The genetic animal model, therefore, provides an opportunity to study disease mechanisms of known pathologies of Muenke syndrome and to test novel/non-invasive therapeutic strategies for them. The genetically equivalent mouse model can also be further explored to discover previously unreported yet potentially significant phenotypes of the syndrome.

Acknowledgments

We thank Drs. Steven R. Twigg and Andrew O. Wilkie (Oxford University, Cambridge, UK) for sharing the *FgfR3*^{P244R} mice with us. The studies on the basicranial synchondrosis and the temporomandibular joint were supported by a grant from NIH/NIAMS to H-D.N. and Mary Downs Endowment Chair Fund to S.P.B. We would like to express our gratitude to our patients for their willingness to take part in ongoing studies at the NIH on Muenke syndrome. These studies were supported in part by the Division of Intramural Research at the National Human Genome Research Institute (National Institutes of Health, Department of Health and Human Services, United States of America).

References

1. Agochukwu NB, Solomon BD, Doherty ES, Muenke M. The palatal and oral manifestations of Muenke syndrome (FGFR3- related craniosynostosis). J Craniofac Surg. 2012 (in press).
2. Bellus GA, Hefferon TW, Ortiz de Luna RI, Hecht JT, Horton WA, Machado M, Kaitila I, McIntosh I, Francomano CA. Achondroplasia is defined by recurrent G380R mutations of FGFR3. Am J Hum Genet. 1995; 56:368–373. [PubMed: 7847369]
3. Bellus GA, McIntosh I, Smith EA, Aylsworth AS, Kaitila I, Horton WA, Greenhaw GA, Hecht JT, Francomano CA. A recurrent mutation in the tyrosine kinase domain of fibroblast growth factor receptor 3 causes hypochondroplasia. Nat Genet. 1995; 10:357–359. [PubMed: 7670477]
4. Bellus GA, Gaudenz K, Zackai EH, Clarke LA, Szabo J, Francomano CA, Muenke M. Identical mutations in three different fibroblast growth factor receptor genes in autosomal dominant craniosynostosis syndromes. Nat Genet. 1996; 14:174–176. [PubMed: 8841188]
5. Boulet SL, Rasmussen SA, Honein MA. A populationbased study of craniosynostosis in metropolitan Atlanta, 1989–2003. Am J Med Genet A. 2008; 146A:984–991. [PubMed: 18344207]
6. Chellaiah AT, McEwen DG, Werner S, Xu J, Ornitz DM. Fibroblast growth factor receptor (FGFR) 3. Alternative splicing in immunoglobulin-like domain III creates a receptor highly specific for acidic FGF/FGF-1. J Biol Chem. 1994; 269:11620–11627. [PubMed: 7512569]

7. Chen L, Li C, Qiao W, Xu X, Deng C. A SeR365)–>Cys mutation of fibroblast growth factor receptor 3 in mouse downregulates Ihh/PTHrP signals and causes severe achondroplasia. Hum Mol Genet. 2001; 10:457–465. [PubMed: 11181569]
8. Collman, H.; Schweitzer, T.; Bohm, H. Imaging studies and neurosurgical treatment. In: Muenke, MKW.; Collman, H.; Solomon, BD., editors. Monographs in Human Genetics Craniosynostoses: Molecular Genetics, Principles of Diagnosis and Treatment. Basel: Karger Publishing; 2011. p. 216-231.
9. Colvin JS, Bohne BA, Harding GW, McEwen DG, Ornitz DM. Skeletal overgrowth and deafness in mice lacking fibroblast growth factor receptor 3. Nat Genet. 1996; 12:390–397. [PubMed: 8630492]
10. de Jong T, Mathijssen IM, Hoogeboom AJ. Additional phenotypic features of Muenke syndrome in 2 Dutch families. J Craniofac Surg. 2011; 22:571–575. [PubMed: 21403557]
11. de Jong T, Toll MS, de Gier HH, Mathijssen IM. Audiological profile of children and young adults with syndromic and complex craniosynostosis. Arch Otolaryngol Head Neck Surg. 2011; 137:775–778. [PubMed: 21844411]
12. Deng C, Wynshaw-Boris A, Zhou F, Kuo A, Leder P. Fibroblast growth factor receptor 3 is a negative regulator of bone growth. Cell. 1996; 84:911–921. [PubMed: 8601314]
13. Doherty ES, Lacbawan F, Hadley DW, Brewer C, Zalewski C, Kim HJ, Solomon B, Rosenbaum K, Domingo DL, Hart TC, Brooks BP, Immken L, Lowry RB, Kimonis V, Shanske AL, Jehee FS, Bueno MR, Knightly C, McDonald-McGinn D, Zackai EH, Muenke M. Muenke syndrome (FGFR3-related craniosynostosis): expansion of the phenotype and review of the literature. Am J Med Genet A. 2007; 143A:3204–3215. [PubMed: 18000976]
14. Escobar LF, Hiett AK, Marnocha A. Significant phenotypic variability of Muenke syndrome in identical twins. Am J Med Genet A. 2009; 149A:1273–1276. [PubMed: 19449410]
15. Fakhry A, Ratisoontorn C, Vedhachalam C, Salhab I, Koyama E, Leboy P, Pacifici M, Kirschner RE, Nah HD. Effects of FGF-2/9 in calvarial bone cell cultures: differentiation stagedependent mitogenic effect, inverse regulation of BMP-2 and noggin, and enhancement of osteogenic potential. Bone. 2005; 36:254–266. [PubMed: 15780951]
16. Glass IA, Chapman S, Hockley AD. A distinct autosomal dominant craniosynostosis-brachydactyly syndrome. Clin Dysmorphol. 1994; 3:215–223. [PubMed: 7981856]
17. Graham JM Jr, Braddock SR, Mortier GR, Lachman R, Van Dop C, Jabs EW. Syndrome of coronal craniosynostosis with brachydactyly and carpal/tarsal coalition due to Pro250Arg mutation in FGFR3 gene. Am J Med Genet. 1998; 77:322–329. [PubMed: 9600744]
18. Harada M, Murakami H, Okawa A, Okimoto N, Hiraoka S, Nakahara T, Akasaka R, Shiraishi Y, Futatsugi N, Mizutani- Koseki Y, Kuroiwa A, Shirouzu M, Yokoyama S, Taiji M, Iseki S, Ornitz DM, Koseki H. FGF9 monomer-dimer equilibrium regulates extracellular matrix affinity and tissue diffusion. Nat Genet. 2009; 41:289–298. [PubMed: 19219044]
19. Honnebier MB, Cabiling DS, Hetlinger M, McDonald-McGinn DM, Zackai EH, Bartlett SP. The natural history of patients treated for FGFR3-associated (Muenke-type) craniosynostosis. Plast Reconstr Surg. 2008; 121:919–931. [PubMed: 18317141]
20. Ibrahimi OA, Zhang F, Eliseenkova AV, Linhardt RJ, Mohammadi M. Proline to arginine mutations in FGF receptors 1 and 3 result in Pfeiffer and Muenke craniosynostosis syndromes through enhancement of FGF binding affinity. Hum Mol Genet. 2004; 13:69–78. [PubMed: 14613973]
21. Jacques BE, Montcouquiol ME, Layman EM, Lewandoski M, Kelley MW. Fgf8 induces pillar cell fate and regulates cellular patterning in the mammalian cochlea. Development. 2007; 134:3021–3029. [PubMed: 17634195]
22. Keller MK, Hermann NV, Darvann TA, Larsen P, Hove HD, Christensen L, Schwartz M, Marsh JL, Kreiborg S. Craniofacial morphology in Muenke syndrome. J Craniofac Surg. 2007; 18:374–386. [PubMed: 17414289]
23. Krejci P, Prochazkova J, Bryja V, Jelinkova P, Pejchalova K, Kozubik A, Thompson LM, Wilcox WR. Fibroblast growth factor inhibits interferon gamma-STAT1 and interleukin 6-STAT3 signaling in chondrocytes. Cell Signal. 2009; 21:151–160. [PubMed: 18950705]

24. Lajeunie E, El Ghouzzi V, Le Merrer M, Munnich A, Bonaventure J, Renier D. Sex related expressivity of the phenotype in coronal craniosynostosis caused by the recurrent P250R FGFR3 mutation. J Med Genet. 1999; 36:9–13. [PubMed: 9950359]
25. Laurita J, Koyama E, Chin B, Taylor JA, Lakin GE, Hankenson KD, Bartlett SP, Nah HD. The Muenke syndrome mutation (FgfR3P244R) causes cranial base shortening associated with growth plate dysfunction and premature perichondrial ossification in murine basicranial synchondroses. Dev Dyn. 2011; 240:2584–2596. [PubMed: 22016144]
26. Madeline LA, Elster AD. Suture closure in the human chondrocranium: CT assessment. Radiology. 1995; 196:747–756. [PubMed: 7644639]
27. Mansour SL, Twigg SR, Freeland RM, Wall SA, Li C, Wilkie AO. Hearing loss in a mouse model of Muenke syndrome. Hum Mol Genet. 2009; 18:43–50. [PubMed: 18818193]
28. Matsunobu T, Torigoe K, Ishikawa M, de Vega S, Kulkarni AB, Iwamoto Y, Yamada Y. Critical roles of the TGF-beta type I receptor ALK5 in perichondrial formation and function, cartilage integrity, and osteoblast differentiation during growth plate development. Dev Biol. 2009; 332:325–338. [PubMed: 19501582]
29. Matsushita T, Wilcox WR, Chan YY, Kawanami A, Bukulmez H, Balmes G, Krejci P, Mekikian PB, Otani K, Yamaura I, Warman ML, Givol D, Murakami S. FGFR3 promotes synchondrosis closure and fusion of ossification centers through the MAPK pathway. Hum Mol Genet. 2009; 18:227–240. [PubMed: 18923003]
30. McBratney-Owen B, Iseki S, Bamforth SD, Olsen BR, Morriss-Kay GM. Development and tissue origins of the mammalian cranial base. Dev Biol. 2008; 322:121–132. [PubMed: 18680740]
31. Minina E, Kreschel C, Naski MC, Ornitz DM, Vortkamp A. Interaction of FGF, Ihh/Pthlh, and BMP signaling integrates chondrocyte proliferation and hypertrophic differentiation. Dev Cell. 2002; 3:439–449. [PubMed: 12361605]
32. Moloney DM, Wall SA, Ashworth GJ, Oldridge M, Glass IA, Francomano CA, Muenke M, Wilkie AO. Prevalence of Pro250Arg mutation of fibroblast growth factor receptor 3 in coronal craniosynostosis. Lancet. 1997; 349:1059–1062. [PubMed: 9107244]
33. Morriss-Kay GM, Wilkie AO. Growth of the normal skull vault and its alteration in craniosynostosis: insights from human genetics and experimental studies. J Anat. 2005; 207:637–653. [PubMed: 16313397]
34. Mueller KL, Jacques BE, Kelley MW. Fibroblast growth factor signaling regulates pillar cell development in the organ of corti. J Neurosci. 2002; 22:9368–9377. [PubMed: 12417662]
35. Muenke M, Schell U. Fibroblast-growth-factor receptor mutations in human skeletal disorders. Trends Genet. 1995; 11:308–313. [PubMed: 8585128]
36. Muenke M, Gripp KW, McDonald-McGinn DM, Gaudenz K, Whitaker LA, Bartlett SP, Markowitz RI, Robin NH, Nwokoro N, Mulvihill JJ, Losken HW, Mulliken JB, Guttmacher AE, Wilroy RS, Clarke LA, Hollway G, Ades LC, Haan EA, Mulley JC, Cohen MM Jr, Bellus GA, Francomano CA, Moloney DM, Wall SA, Wilkie AO, et al. A unique point mutation in the fibroblast growth factor receptor 3 gene (FGFR3) defines a new craniosynostosis syndrome. Am J Hum Genet. 1997; 60:555–564. [PubMed: 9042914]
37. Murakami S, Kan M, McKeehan WL, de Crombrugghe B. Up-regulation of the chondrogenic Sox9 gene by fibroblast growth factors is mediated by the mitogen-activated protein kinase pathway. Proc Natl Acad Sci U S A. 2000; 97:1113–1118. [PubMed: 10655493]
38. Naski MC, Wang Q, Xu J, Ornitz DM. Graded activation of fibroblast growth factor receptor 3 by mutations causing achondroplasia and thanatophoric dysplasia. Nat Genet. 1996; 13:233–237. [PubMed: 8640234]
39. Naski MC, Colvin JS, Coffin JD, Ornitz DM. Repression of hedgehog signaling and BMP4 expression in growth plate cartilage by fibroblast growth factor receptor 3. Development. 1998; 125:4977–4988. [PubMed: 9811582]
40. Okamoto K, Ito J, Tokiguchi S, Furusawa T. High-resolution CT findings in the development of the sphenooccipital synchondrosis. AJNR Am J Neuroradiol. 1996; 17:117–120. [PubMed: 8770261]

41. Ornitz DM, Xu J, Colvin JS, McEwen DG, MacArthur CA, Coulier F, Gao G, Goldfarb M. Receptor specificity of the fibroblast growth factor family. J Biol Chem. 1996; 271:15292–15297. [PubMed: 8663044]
42. Pickles JO. The expression of fibroblast growth factors and their receptors in the embryonic and neonatal mouse inner ear. Hear Res. 2001; 155:54–62. [PubMed: 11335076]
43. Reardon W, Wilkes D, Rutland P, Pulleyn LJ, Malcolm S, Dean JC, Evans RD, Jones BM, Hayward R, Hall CM, Nevin NC, Baraister M, Winter RM. Craniosynostosis associated with FGFR3 pro250arg mutation results in a range of clinical presentations including unisutural sporadic craniosynostosis. J Med Genet. 1997; 34:632–636. [PubMed: 9279753]
44. Rice DP, Rice R, Thesleff I. Fgfr mRNA isoforms in craniofacial bone development. Bone. 2003; 33:14–27. [PubMed: 12919696]
45. Ridgway EB, Wu JK, Sullivan SR, Vasudavan S, Padwa BL, Rogers GF, Mulliken JB. Craniofacial growth in patients with FGFR3Pro250Arg mutation after fronto-orbital advancement in infancy. J Craniofac Surg. 2011; 22:455–461. [PubMed: 21403567]
46. Rousseau F, Bonaventure J, Legeai-Mallet L, Pelet A, Rozet JM, Maroteaux P, Le Merrer M, Munnich A. Mutations in the gene encoding fibroblast growth factor receptor-3 in achondroplasia. Nature. 1994; 371:252–254. [PubMed: 8078586]
47. Sabatino G, Di Rocco F, Zampino G, Tamburrini G, Caldarelli M, Di Rocco C. Muenke syndrome. Childs Nerv Syst. 2004; 20:297–301. [PubMed: 14963686]
48. Shim K, Minowada G, Coling DE, Martin GR. Sprouty2, a mouse deafness gene, regulates cell fate decisions in the auditory sensory epithelium by antagonizing FGF signaling. Dev Cell. 2005; 8:553–564. [PubMed: 15809037]
49. Thomas GP, Wilkie AO, Richards PG, Wall SA. FGFR3 P250R mutation increases the risk of reoperation in apparent ‘non-syndromic’ coronal craniosynostosis. J Craniofac Surg. 2005; 16:347–352. discussion 353–344. [PubMed: 15915095]
50. Twigg SR, Healy C, Babbs C, Sharpe JA, Wood WG, Sharpe PT, Morriss-Kay GM, Wilkie AO. Skeletal analysis of the Fgfr3 (P244R) mouse, a genetic model for the Muenke craniosynostosis syndrome. Dev Dyn. 2009; 238:331–342. [PubMed: 19086028]
51. Wilkie AO, Oldridge M, Tang Z, Maxson RE Jr. Craniosynostosis and related limb anomalies. Novartis Found Symp. 2001; 232:122–133. discussion 133–143. [PubMed: 11277076]
52. Wilkie AO, Byren JC, Hurst JA, Jayamohan J, Johnson D, Knight SJ, Lester T, Richards PG, Twigg SR, Wall SA. Prevalence and complications of single-gene and chromosomal disorders in craniosynostosis. Pediatrics. 2010; 126:e391–e400. [PubMed: 20643727]
53. Wu XL, Gu MM, Huang L, Liu XS, Zhang HX, Ding XY, Xu JQ, Cui B, Wang L, Lu SY, Chen XY, Zhang HG, Huang W, Yuan WT, Yang JM, Gu Q, Fei J, Chen Z, Yuan ZM, Wang ZG. Multiple synostoses syndrome is due to a missense mutation in exon 2 of FGF9 gene. Am J Hum Genet. 2009; 85:53–63. [PubMed: 19589401]
54. Yasuda T, Nah HD, Laurita J, Kinumatsu T, Shibukawa Y, Shibutani T, Minugh-Purvis N, Pacific M, Koyama E. Muenke syndrome mutation, FgfR3(P244R), causes TMJ defects in postnatal mice. J Dent Res. 2012 (in press).
55. Zhang R, Murakami S, Coustry F, Wang Y, de Crombrugghe B. Constitutive activation of MKK6 in chondrocytes of transgenic mice inhibits proliferation and delays endochondral bone formation. Proc Natl Acad Sci U S A. 2006; 103:365–370. [PubMed: 16387856]
56. Zhou G, Schwartz LT, Gopen Q. Inner ear anomalies and conductive hearing loss in children with Apert syndrome: an overlooked otologic aspect. Otol Neurotol. 2009; 30:184–189. [PubMed: 19169132]

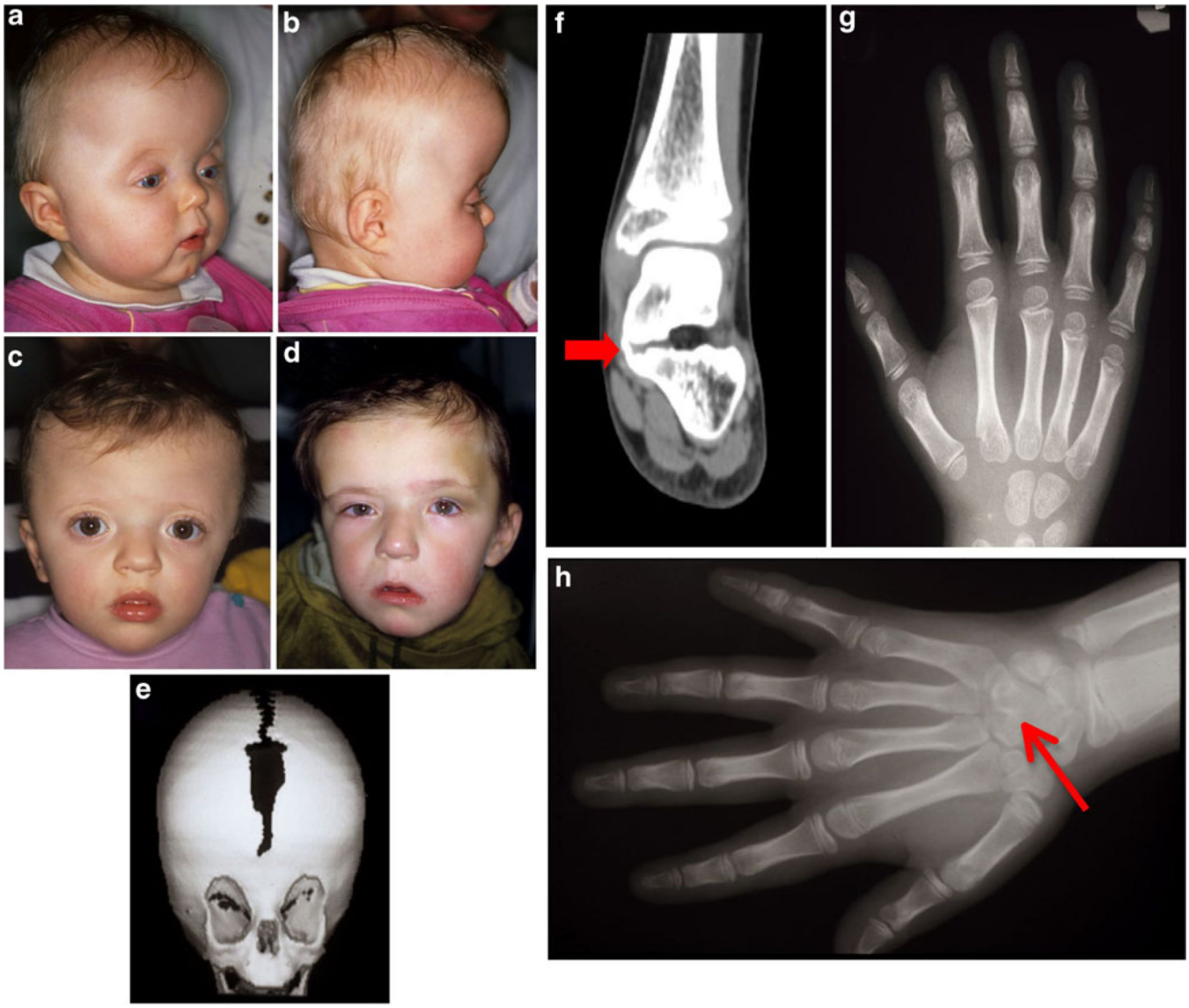

Fig. 1.

a–d Pre-operative photos of patients with Muenke syndrome. **a, b** An 11-month-old patient with Muenke syndrome with turribrachycephaly, and a bulging forehead; **c** 16-month-old patient with Muenke syndrome, showing brachycephaly, with a high forehead, bulging temporal squama, and mild hypertelorism; **d** 45-month-old patient, showing anterior plagiocephaly due to left unilateral coronal synostosis; **e** three-dimensional reformatted computed tomography of a 4-month-old (same patient as **c**), demonstrating brachycephaly and incomplete midline ossification, as well as a shortened anterior cranial base; **f** tarsal bone fusion (talus-calcaneus) in a patient with Muenke syndrome (*red arrow*) (female, 7 years); **g** thimble-like intermediate second phalanx with cone-shaped epiphysis and an abnormally short intermediate fifth phalanx (female, 7 years); **h** carpal bone fusion (capitate-hamate) in a patient with Muenke syndrome (*red arrow*). (*Photos* **a–e, g, h***: courtesy of H. Collmann, and published with consent from participating patients*)

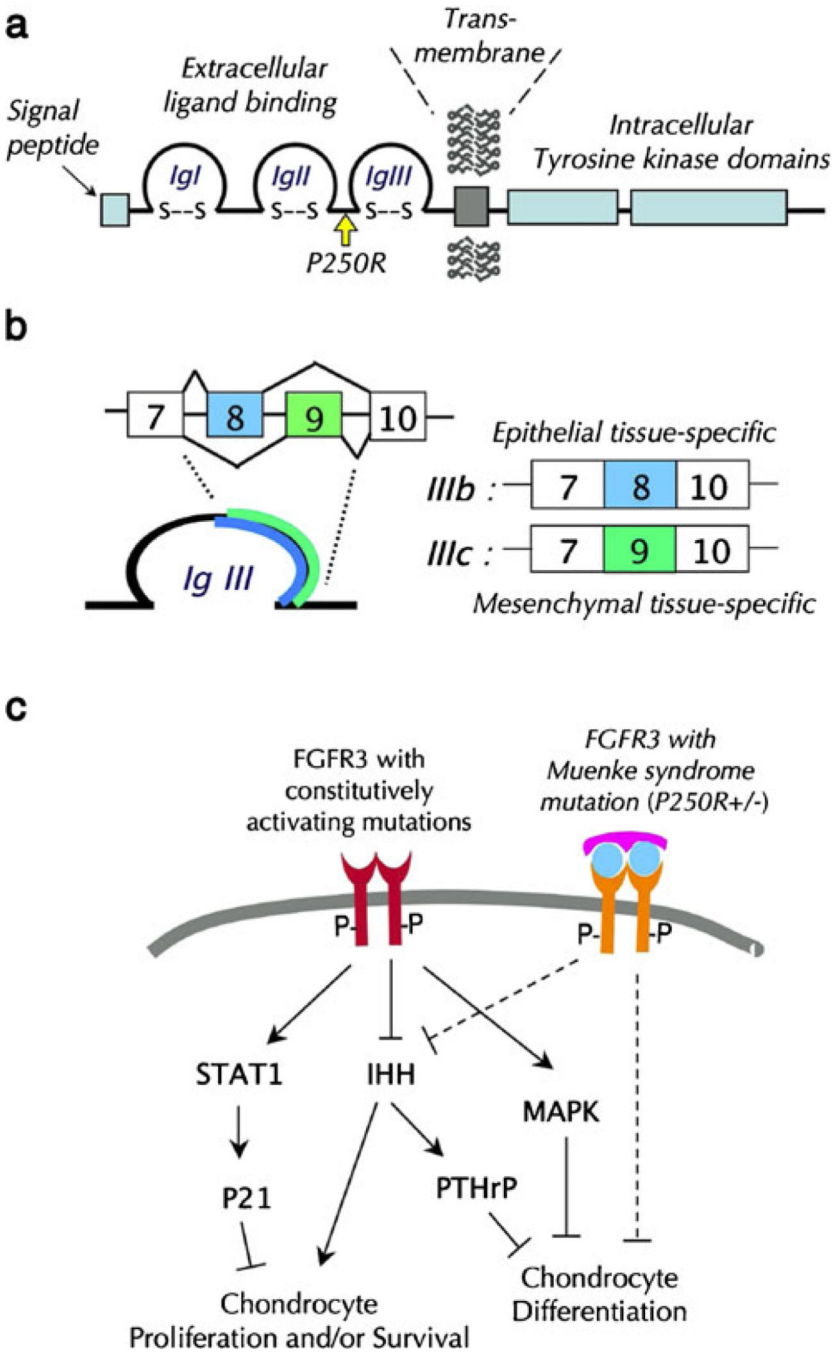

Fig. 2.

a A schematic diagram depicting the FGFR3 protein domains and the location of the Muenke syndrome mutation. **b** Alternatively splicing of exons 8 and 9 of the *FGFR3* gene results in epithelia; tissuespecific IIIb isoform and mesenchymal tissue-specific IIIc isoforms. **c** Constitutively activating ligand-independent mutations of FGFR3 inhibit chondrogenic cell proliferation and/or survival and differentiation via activation of STAT1 [23], inhibition of IHH signaling [7], and sustained activation of MAPK [37, 55].

TheMuenke syndrome mutation, a ligand-dependent activating mutation, inhibits chondrocyte proliferation via IHH signaling and inhibits chondrocyte maturation [25, 54]

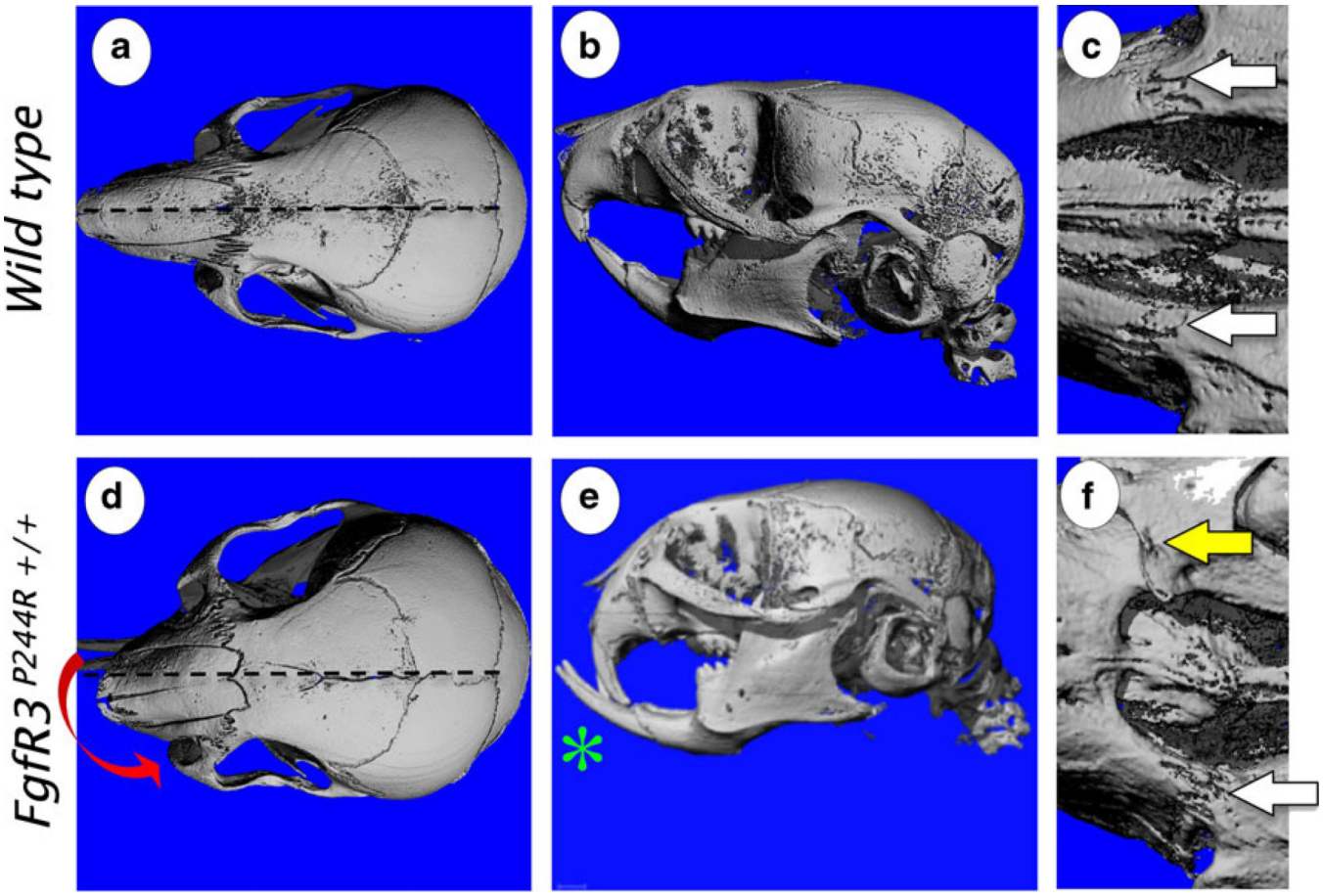

Fig. 3.

Micro-CT of the 3-week-old wild-type control (**a–c**) and *FgfR3*^{P244R} mutant (**d–f**) mouse skulls. Homozygous mutant mice (*FgfR3*$^{P244R+/+}$) display shortening of the snout and Class III malocclusion of incisors (*green asterisk*) (**e**), correlating with fusion of premaxillary sutures (*yellow arrows*) (**f**). The *white arrow* points patent premaxillary sutures (**c, f**). Skewing of the snout (*red arrow*) is visible in some 3-week-old mutant mice (**d**). Age-matched wild-type mice did not show any of these phenotypes (**a–c**). *(Adopted from Developmental Dynamics 240(11):2584–2594, 2011)*

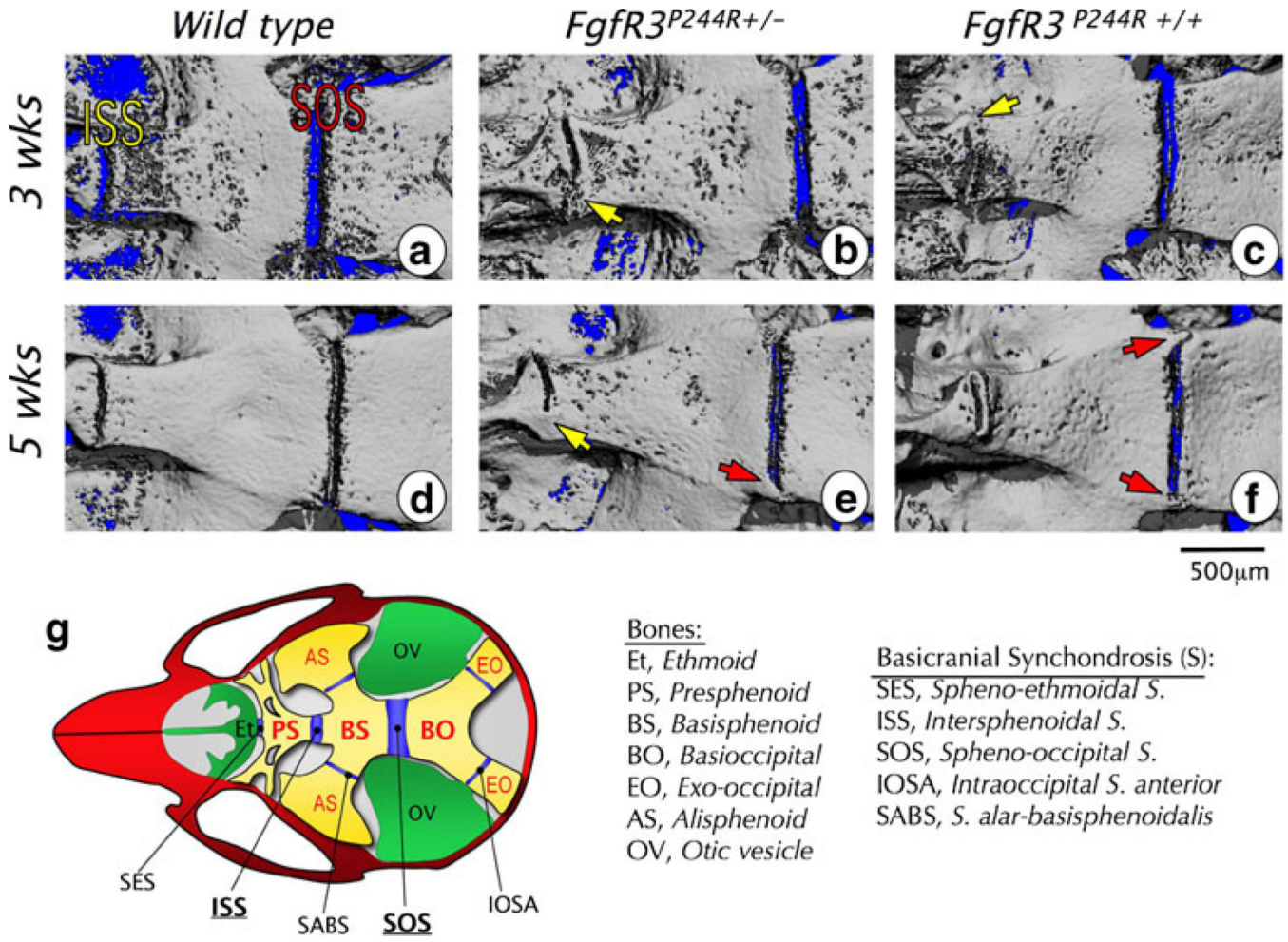

Fig. 4.

Micro-CT images of basicranial synchondrosis closure in wild-type and heterozygous (*FgfR3*$^{P244R+/-}$) and homozygous (*FgfR3*$^{P244R+/+}$) mutant mice. **a–f** Skull bases of wild-type (**a, d**), heterozygous mutant (**b, e**), and homozygous mutant (**c, f**) mice are imaged at 3 weeks (**a–c**) and 5 weeks (**d–f**). In all images, *left* is rostral and *right* is caudal. Bridged or closed intersphenoidal synchondrosis (ISS) is indicated with a *yellow arrow* and the bridged or closed spheno-occipital synchondrosis (SOS) with a *red arrow*. Scale bar0500 µm. **g** The diagram illustrates locations of and relationships among synchondroses and bones in the cranial base. *(Adopted from Developmental Dynamics 240(11):2584–2594, 2011)*

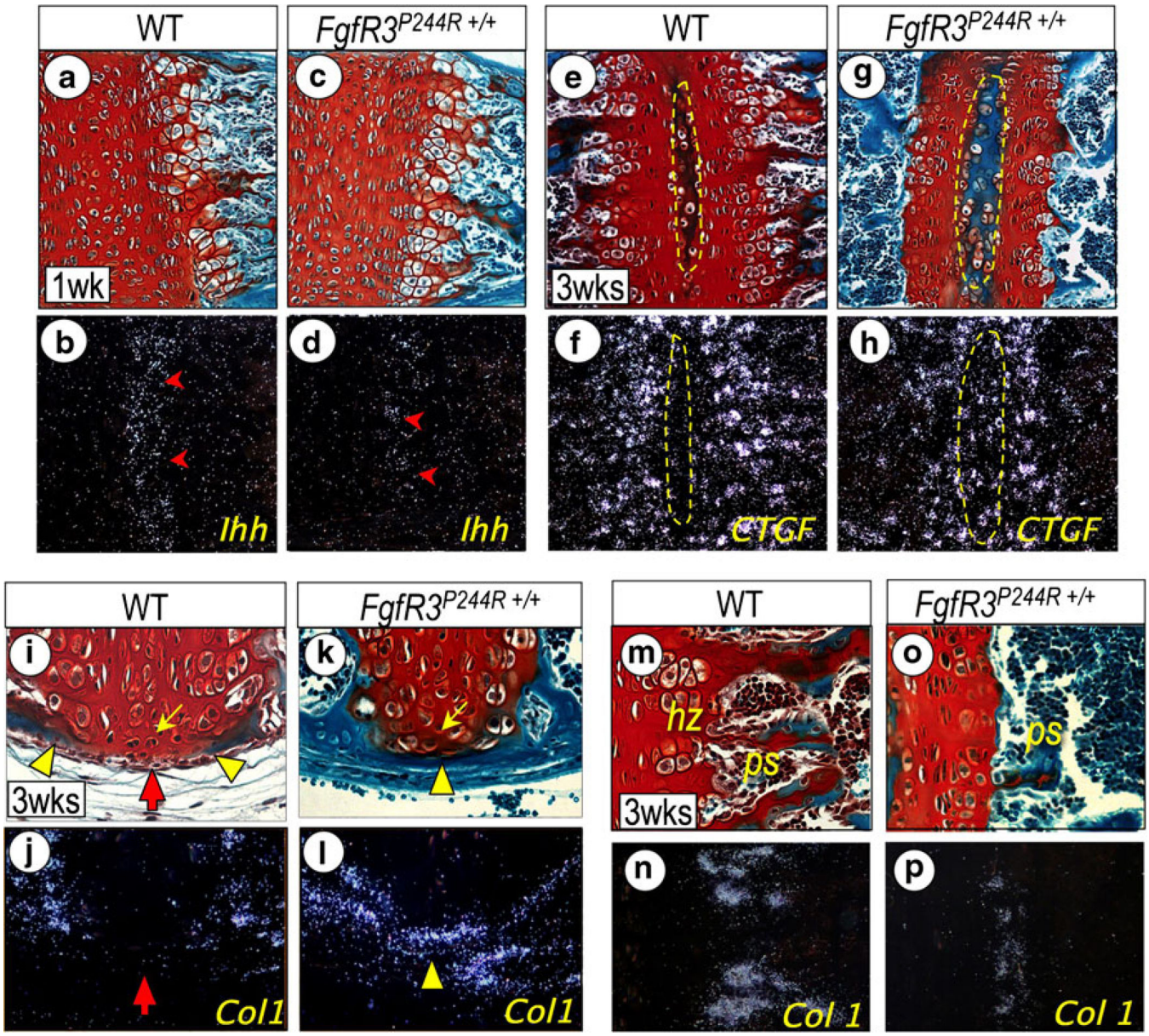

Fig. 5.

Endochondral ossification (**a–d**), secondary ossification center development (**e–h**), perichondrial ossification (**i–l**), and primary spongiosa bone formation (**m–p**) are shown in wild-type *FgfR3*$^{P244R+/+}$ mutant basicranial synchondroses. Parasagittal serial sections of intersphenoidal synchondrosis (ISS) from 3-week-old wild-type (**i, j**) and mutant (**k, l**), and spheno-occipital synchondroses (SOS) from 1-week-(**a–d**) and 3-week-old (**e–n**) wild-type (**a, b, e, f, m, n**) and mutant (**c, d, g, h, o, p**) mice were processed for staining with fast green/Safranin O (**a, c, e, g, i, k, m**) and in situ hybridization with the indicated genes (**b, d, f, h, j, l, n**). Notice the marked reduction of *Ihh* expression in the prehypertrophic zone (**d**, *arrowhead*) in mutant SOS. Note also that, in 3-week-old mutant SOS, the shortened growth plate is accompanied with the accelerated development of the secondary ossification center (**e, g**); indicated with a dotted *yellow circle*), which is recognizable by the activation of

CTGF (**h**). Precocious perichondrial ossification is visible in the ISS from 3-week-old mutant as shown by fast green staining (**k**) and in situ hybridization with Type I collagen (*Col 1*; **l**) along the entire length of the synchondrosis cartilage. In wild-type ISS, the perichondrium flanking resting chondrocytes (*yellow arrow*) remains unossified (*red arrow*) at this time, as indicated by the lack of *Col1* and other osteogenic gene (data not shown) expression (**i, j**). Notice that the chondrocytes flanking the perichondrium in mutant ISS have the appearance of prehypertrophic chondrocytes (**k**, *yellow arrow*). Notice the significant reduction of hypertrophic chondrocyte zone (*hz*) and primary spongiosa (*ps*) at the chondro-osseous border in 3-week-old mutant SOS (**o**) compared with wild-type SOS (**l**), which is identifiable by the significant reduction of *Col 1* (**m, p**). Other genes required for chondro-osseous transition are also drastically reduced (data not shown). *(Adopted from Developmental Dynamics 240 (11):2584–2594, 2011)*

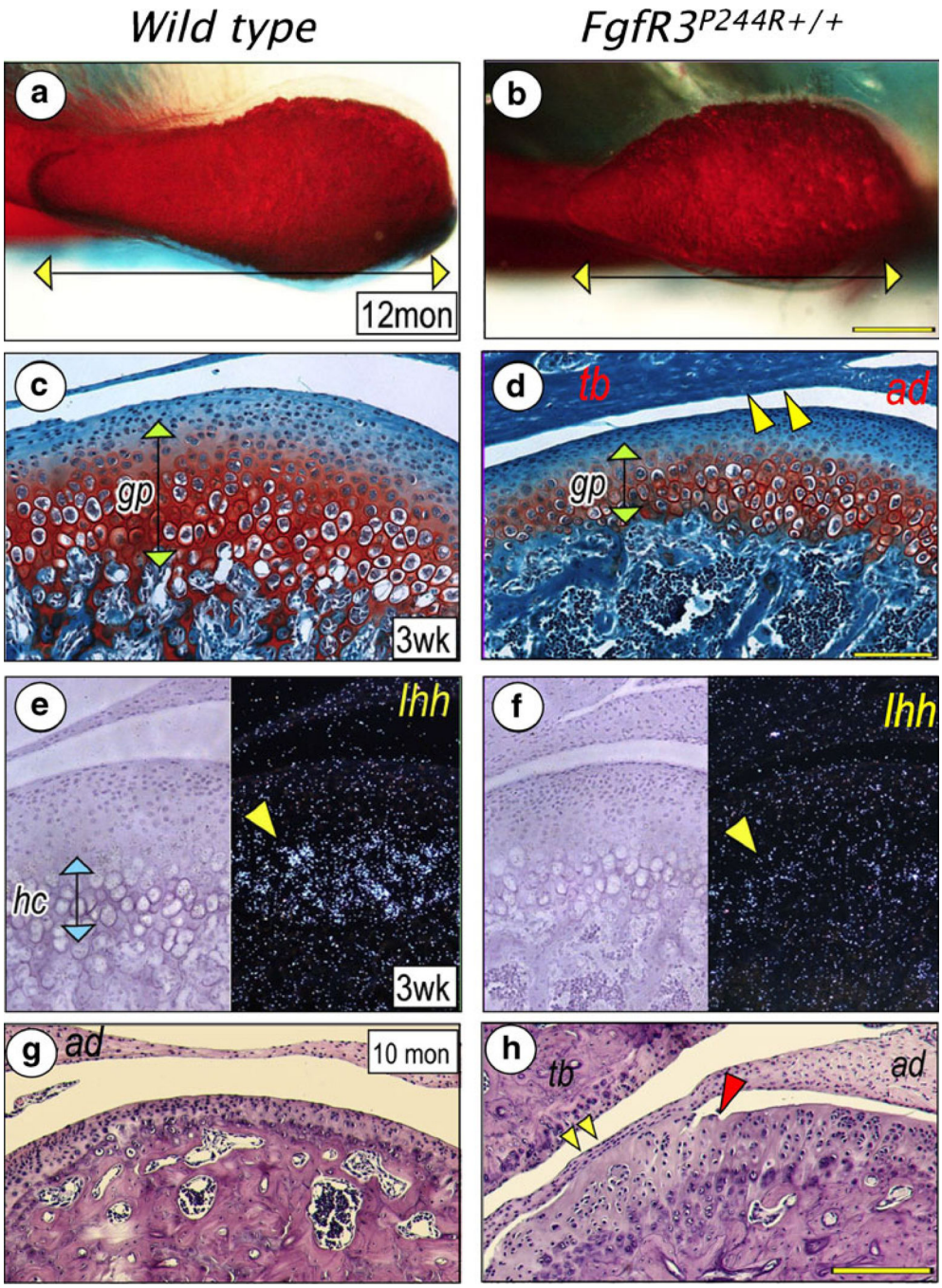

Fig. 6.

Defective development and arthritic changes of the temporomandibular joint in *FgfR3*^{P244R} mutant mice. A superior view of the condylar head shows that the mesial half is nearly absent in the mutant mice (**b**) compared with a wild type (**a**). The mutant mice also show significantly reduced growth plate-like cartilage (*gp*) of the mandibular condyle (**d**) and *Ihh* expression in hypertrophying chondrocytes (*hc*) (**f**), compared to a wild type (**c, e**). Articular discs (*ad*) of the mutant mice adhere to articular eminence of the temporal bone (*tb*) (**d**, *yellow arrowheads*) or condylar surface (**h**, *yellow arrowheads*). Also, the articular surface

of the mutant condyle presents fissure formation (**h**), *red arrowhead*). Neither disc adhesion nor fissure formation are observed in wild type (**c,g**). *(Adopted from J Dent Res, 2012)*